



## Ex situ and in situ characterization studies of spin-coated TiO<sub>2</sub> film electrodes for the electrochemical ozone production process

Kenta Kitsuka<sup>a,b</sup>, Kazuhiro Kaneda<sup>a</sup>, Mineo Ikematsu<sup>a</sup>, Masahiro Iseki<sup>a</sup>,  
Katsuhiko Mushiake<sup>a</sup>, Takeo Ohsaka<sup>b,\*</sup>

<sup>a</sup> Eco Technology Research Center, Sanyo Electric Co., Ltd., 1-1-1 Sakata, Oizumi, Ora, Gunma 370-0596, Japan

<sup>b</sup> Department of Electronic Chemistry, Interdisciplinary Graduate School of Science and Engineering, Tokyo Institute of Technology, 4259 Nagatsuta, Midori-ku, Yokohama 226-8502, Japan

### ARTICLE INFO

#### Article history:

Received 6 May 2009

Received in revised form 14 July 2009

Accepted 19 July 2009

Available online 28 July 2009

#### Keywords:

TiO<sub>2</sub>

Semiconductor electrode

Water electrolysis

Electrochemical ozone production

Spin-coating

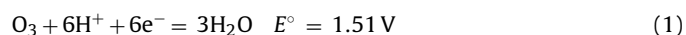
### ABSTRACT

An electrode composed of silicon/titanium oxide/platinum/titanium dioxide (Si/TiO<sub>x</sub>/Pt/TiO<sub>2</sub>) was fabricated by spin-coating TiO<sub>2</sub> multilayers on a Si/TiO<sub>x</sub>/Pt substrate and was used in electrochemical ozone production (EOP). EOP was realized when the Si/TiO<sub>x</sub>/Pt substrate was completely covered with the TiO<sub>2</sub> film and a current efficiency of 7% was achieved at a low current density of 26.7 mA cm<sup>-2</sup> in 0.01 M HClO<sub>4</sub> at 15 °C. The TiO<sub>2</sub> film was found to be of an anatase-type TiO<sub>2</sub> and that to comprise aperture structures from the X-ray diffraction (XRD) and transmission electron microscopy (TEM) observations. Moreover, the fabricated TiO<sub>2</sub> film was found to be an n-type semiconductor by photoelectrochemical measurements. The high efficiency at a low current density of EOP on the TiO<sub>2</sub> n-type semiconductor was explained to result from the electron transfer through the TiO<sub>2</sub>/HClO<sub>4</sub> interface as tunneling current. When the tunneling current passes through a depletion layer of TiO<sub>2</sub>, the electrode potential is necessarily high enough to facilitate EOP.

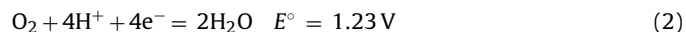
© 2009 Elsevier Ltd. All rights reserved.

### 1. Introduction

Ozone is a very strong oxidant (Eq. (1),  $E^\circ = 1.51$  V vs. SHE) and its decomposition leads to environmentally friendly products (O<sub>2</sub>) and thus O<sub>3</sub> finds applications in many fields such as water treatment, clean-up of effluents and bleaching of wood pulp [1,2]:



The low ozone concentration available using corona discharge or UV-light absorption technologies restricts ozone application where a higher ozone concentration is necessary [1,2]. To overcome this difficulty, the alternative technology of electrochemical ozone production (EOP) from water electrolysis has been studied extensively [1–20]. The electrode materials and the electrolyte composition are critical to determine the ozone production efficiency. This efficiency is closely related to oxygen evolution reaction (OER, Eq. (2)), which is thermodynamically favored over EOP:



Consequently, for EOP, the electrode material is required to possess a high overpotential for OER. For this purpose, many anode

materials, which in general have a wide potential window and a high oxygen overpotential, such as Pt [3,4,11], boron-doped diamond (BDD) [12] and lead dioxide (PbO<sub>2</sub>) [1–10] have been studied previously together with various electrolyte solutions. Pt has the highest oxygen overpotential among the noble metals and their alloys, and therefore, it has traditionally been used in EOP. However, it does not necessarily have a high ozone production efficiency (e.g., less than 2% at a current density of 400 mA cm<sup>-2</sup> [3]). On the other hand, a p-type semiconductor BDD has a wide electrochemical potential window and also a high oxygen overpotential. However, it is not used widely in EOP due to its high cost and/or low ozone production efficiency at low current densities.

PbO<sub>2</sub>, a cheap electrode material possessing a relatively high overpotential for OER, is the best candidate for EOP and for example, a current efficiency of 6–7% for ozone production was reported at a relatively low current density of 50 mA cm<sup>-2</sup> in a phosphate buffer at room temperature [5]. As a result, up to now most of the investigations have centered on PbO<sub>2</sub>; the influences of supporting electrolyte [1,3,6–8], temperature [2,6–8] and power consumption [1,7] for EOP were studied. Also, the ozone production mechanisms [1,2,7–9] and kinetics [1,7,9] using PbO<sub>2</sub> electrodes were investigated in detail. However, the use of lead-containing materials for EOP, e.g., for water sterilization is not recommended because of the dissolution of poisonous lead species.

In our previous studies [15–17], we have discussed ozone electrogeneration using tantalum oxide (TaO<sub>x</sub>) and Pt composite-

\* Corresponding author. Tel.: +81 45 924 5404; fax: +81 45 924 5489.  
E-mail address: [ohsaka@chem.titech.ac.jp](mailto:ohsaka@chem.titech.ac.jp) (T. Ohsaka).

coated Ti electrodes in model tap water in which the catalyst layer composed of insulating TaO<sub>x</sub> and metallic Pt was fabricated by thermal decomposition. Further, we have also investigated the function of the TaO<sub>x</sub> insulator thin film, which was fabricated by the RF sputtering method on a Si/Pt substrate, as a catalyst of ozone production in model tap water [18] and in 0.1 M perchloric acid (HClO<sub>4</sub>) [19], in which its high oxygen overpotential was found to originate from the TaO<sub>x</sub> band structure and a high current efficiency at a low current density for ozone production (8% at 10 mA cm<sup>-2</sup>) was achieved. Thus, a TaO<sub>x</sub> thin film is an excellent electrode material for EOP. However, Ta is comparatively expensive when compared to other industrial materials. Recently, we have found a superior electrocatalysis of low-priced titanium oxides for EOP and have reported the preliminary results on EOP [20]. In the present study, we fabricated the electrodes composed of silicon/titanium oxide/platinum/titanium dioxide (Si/TiO<sub>x</sub>/Pt/TiO<sub>2</sub>) with TiO<sub>2</sub> films of various thicknesses (approximately 50–800 nm). The TiO<sub>2</sub> thin films were spin-coated on Si/TiO<sub>x</sub>/Pt substrates, and their electrochemical and photoelectrochemical properties as well as their EOP activity were examined in detail. In addition, the obtained EOP results are successfully explained by considering the band structure of the n-type TiO<sub>2</sub>/HClO<sub>4</sub> solution interface.

## 2. Experimental

### 2.1. Preparation of Si/TiO<sub>x</sub>/Pt/TiO<sub>2</sub> electrode

Fig. 1 shows the cross-sectional structure of the fabricated electrode. The Si substrate was placed inside the chamber of the RF sputtering unit (ULVAC). A TiO<sub>x</sub> film (thickness: ca. 50 nm) was deposited on the Si substrate. The TiO<sub>x</sub> layer acted as a binding agent between the Si substrate (thickness: 1 mm) and the subsequent Pt layer (thickness: ca. 500 nm), thereby increasing the durability of the electrode. It also suppressed the mutual diffusion of the Si and Pt layers. The Pt layer was deposited onto the TiO<sub>x</sub> film, hitherto deposited on the Si substrate, by sputtering. Finally, the precursor of TiO<sub>2</sub> (Ti-03, Kojundo Chemical Laboratory) was spin-coated (ACT-450A, Active) on the Pt at 500 rpm for 5 s, then at 3000 rpm for 10 s. After spin-coating, the electrode was dried at room temperature (10 min), 200 °C (10 min) and then calcined at 600 °C in air (10 min). The sample electrodes were fabricated by 1–18 times repeating the sequence for the surface TiO<sub>2</sub> layer (approximately 50–800 nm). The fabricated Si/TiO<sub>x</sub>/Pt/TiO<sub>2</sub> was positioned on the Ti substrate and the Pt layer of the Si/TiO<sub>x</sub>/Pt/TiO<sub>2</sub> was contacted to the Ti substrate using Ag paste. Then the surface TiO<sub>2</sub> film was covered with a fluorine resin tape with geometric area of 2.25 cm<sup>2</sup>.

### 2.2. Ozone production

A cell divided by a cation-exchange membrane (Nafion®) was used for the evaluation of ozone production. A 0.01 M HClO<sub>4</sub> (pH 2.0) was used as the electrolyte solution, and the solution temperature was maintained at 15 °C. The Si/TiO<sub>x</sub>/Pt/TiO<sub>2</sub> electrode and a Pt plate were used as the anode and the cathode, respectively, and the distance between the anode and the cathode was maintained constant (1 cm). A constant-current electrolysis at 60 mA

(26.7 mA cm<sup>-2</sup>) was performed for 5 min. The concentration of ozone which was electrogenerated and partitioned in the electrolyte solution phase was measured by colorimetry (DR/4000U, HACH), and the amount of ozone gas partitioned in gas phase (i.e., liberated from the electrolyzed solution) was not determined. Therefore, it should be noted that “the current efficiency for EOP” used in this study is based on the amount of ozone partitioned in the electrolyte solution.

### 2.3. Characterization of the electrode

The thickness of the TiO<sub>2</sub> films was determined by X-ray fluorescence (XRF) spectrometric analysis using the fundamental parameter method (JSX-3220ZS, JEOL). The crystal structures of the samples were determined by grazing incidence X-ray diffraction (XRD) operated with Cu Kα (λ = 1.54056 Å) radiation at 45 kV and 360 mA (D8-DISCOVER, Bruker AXS). Atomic force microscopy (AFM) was used to observe the surface structure of the TiO<sub>2</sub> films (SPM-9600, Shimadzu). Transmission electron microscopy (TEM) was operated at 200 keV to observe the cross-sections of the TiO<sub>2</sub> films (JEM-2100F, JEOL).

### 2.4. Electrochemical measurements

Cyclic voltammetry (CV) and steady-state polarization measurements were performed in a conventional three-electrode cell made of Pyrex glass with a potentiostat/galvanostat (HZ-3000, Hokuto Denko) at 24 °C. In this case, the raw data of the polarization measurements were corrected for the so-called ohmic drop using a current interrupter method [21].

The counter and reference electrodes were a platinum mesh and Ag/AgCl (sat. KCl), respectively. The electrolyte (HClO<sub>4</sub>, 0.01 and 0.1 M) was saturated with N<sub>2</sub> prior to electrochemical measurements.

The photoelectrochemical properties were measured under irradiation from a Xe lamp (300 W) with the wavelength of the light was in the range of 185–2000 nm. A quartz cell was used for action spectra measurements, in which the working, counter and Ag/AgCl (sat. KCl) reference electrodes were set using an aqueous solution of 0.1 M HClO<sub>4</sub> (pH 1.0). The reference electrode was shielded to prevent the irradiation from the Xe lamp.

## 3. Results and discussion

### 3.1. Thickness of TiO<sub>2</sub> and ozone production

Fig. 2 shows the relationship between the thickness of the surface TiO<sub>2</sub> film and the number of spin-coatings. The film thickness

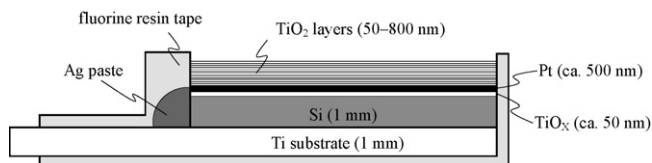


Fig. 1. Cross-sectional structure of the Si/TiO<sub>x</sub>/Pt/TiO<sub>2</sub> electrode.

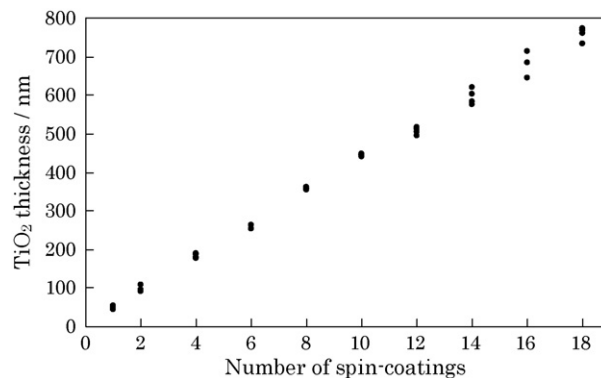
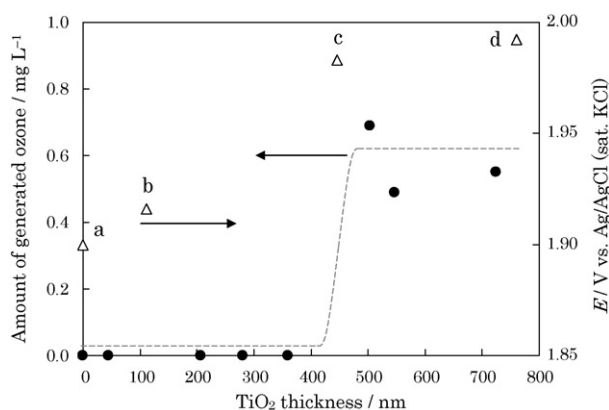


Fig. 2. Relationship between the thickness of the surface TiO<sub>2</sub> film and the number of spin-coating. Three to four samples were measured at each number of spin-coating.



**Fig. 3.** Relationship between the TiO<sub>2</sub> film thickness and the amount of generated ozone in 0.01 M HClO<sub>4</sub> at 15 °C. Points (a–d) represent the electrode potential of Si/TiO<sub>x</sub>/Pt/TiO<sub>2</sub> electrodes with TiO<sub>2</sub> films of different thicknesses during the electrolysis at 60 mA. The data were taken from Fig. 4.

was found to increase almost proportionally with an increase in the number of spin-coatings; a TiO<sub>2</sub> film of ca. 45 nm was obtained by carrying out onetime spin-coating. Thus, we could prepare the TiO<sub>2</sub> films of an arbitrarily controlled thickness in the examined range of 50–800 nm. In Fig. 3 is shown the dependence of the amount of the electrogenerated ozone on the thickness of the surface TiO<sub>2</sub> film from 0 to 724 nm. Ozone production was observed when the film thickness of the TiO<sub>2</sub> film was greater than approximately 500 nm. Assuming that the EOP reaction consumes six electrons ( $3\text{H}_2\text{O} = \text{O}_3 + 6\text{H}^+ + 6\text{e}^-$ ), the current efficiency of approximately 7% was achieved at the 500-nm thickness TiO<sub>2</sub> film. On the other hand, EOP was not realized when a TiO<sub>2</sub> film of thickness less than 400 nm was used.

### 3.2. Electrochemical measurements

Fig. 4 shows the steady-state polarization curves for the electrolytic oxidation of H<sub>2</sub>O using Si/TiO<sub>x</sub>/Pt/TiO<sub>2</sub> electrodes with various thicknesses (*l*) of the TiO<sub>2</sub> film in 0.1 M HClO<sub>4</sub> solution at 24 °C, in which the polarization curves were corrected for ohmic drop using a current interrupter procedure [21]. In each case, the electrolysis was carried out galvanostatically, and the electrode potential was measured at 2 min after the beginning of the electrolysis. The obtained polarization curves varied with the thickness of TiO<sub>2</sub> films. The curves (c) (*l* = 446 nm) and (d) (*l* = 760 nm) show a larger overpotential for the electrolytic oxidation of water than

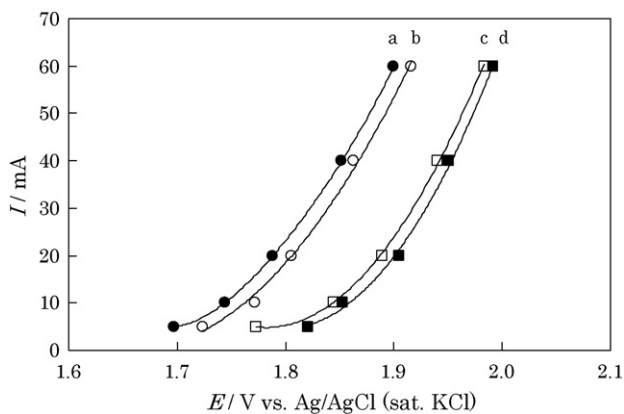


**Fig. 4.** Steady-state polarization curves obtained at Si/TiO<sub>x</sub>/Pt/TiO<sub>2</sub> electrodes with different thicknesses of TiO<sub>2</sub> films ((a) 0 nm, (b) 112 nm, (c) 446 nm, (d) 760 nm) in 0.1 M HClO<sub>4</sub> solution at 24 °C.

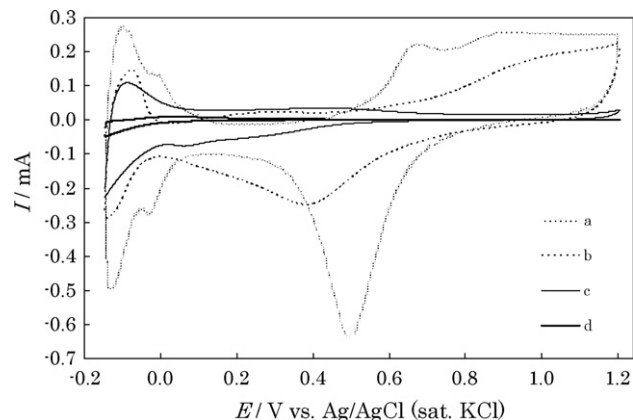


**Fig. 5.** Cyclic voltammograms obtained at Si/TiO<sub>x</sub>/Pt/TiO<sub>2</sub> electrodes with different thicknesses of TiO<sub>2</sub> films ((a) 0 nm, (b) 350 nm, (c) 440 nm and (d) 760 nm) in 0.01 M HClO<sub>4</sub> solution under N<sub>2</sub> atmosphere at 24 °C. Potential scan rate: 100 mV s<sup>-1</sup>.

the curves (a) (*l* = 0 nm) and (b) (*l* = 112 nm), e.g., as shown in Fig. 3, the electrode potentials (at 60 mA) of the electrodes c and d are approximately 0.1 V more positive than those of the electrodes a and b. In addition, possibly in close relation to this fact, it is obvious from the thickness dependence of EOP that the electrodes with the TiO<sub>2</sub> films of more than ca. 440 nm (i.e., prepared by repeating the spin-coating 10 times) possess a significant ozone production efficiency, while the electrodes with the films of thickness less than ca. 440 nm do not actually produce ozone.

The cyclic voltammograms shown in Fig. 5 were obtained at the Si/TiO<sub>x</sub>/Pt/TiO<sub>2</sub> electrodes with various thicknesses of TiO<sub>2</sub> film with a common geometric area of 2.25 cm<sup>2</sup>. In curve (a), the characteristic CV response of the Pt electrode is shown; the formation of Pt oxide layer ( $E > 0.6$  V) and its reduction as the cathodic peak at 0.5 V, the double layer region ( $0.1 < E < 0.5$  V) and the hydrogen adsorption/desorption ( $-0.15 < E < 0$  V). The voltammogram of the electrode with a 350 nm TiO<sub>2</sub> film is shown in Fig. 5(b). In this case, the ill-defined CV response corresponding to the formation of the Pt oxide layer and its reduction and the hydrogen adsorption/desorption is observed. As TiO<sub>2</sub> is considered to be electrochemically inert in this potential range [22], the response in curve (b) is considered to be ascribed to the Pt substrate below the TiO<sub>2</sub> film. The voltammogram of the electrode with a 440 nm TiO<sub>2</sub> film is shown in Fig. 5(c). In this case, the ill-defined and much smaller CV response is observed, compared with curve (b). Furthermore, the electrode with 760 nm TiO<sub>2</sub> film gave an almost featureless CV response (see curve (d)). By combining these CV responses obtained at the electrodes with various thicknesses of TiO<sub>2</sub> films with the TiO<sub>2</sub> thickness-dependent ozone production (Fig. 3), we can consider that the electrodes completely covered with TiO<sub>2</sub> films are promising as anode materials for EOP and at the same time the TiO<sub>2</sub> film exhibits a good activity for EOP.

### 3.3. Characterizations of the surface TiO<sub>2</sub> film

The XRD patterns of the electrodes with varying thicknesses of TiO<sub>2</sub> films in the range 50–720 nm are shown in Fig. 6. The assignment of each peak is also indicated in the figure. All the diffraction peaks of each electrode are ascribed to anatase TiO<sub>2</sub> (●) and the Pt (○) substrate of Si/TiO<sub>x</sub>/Pt. The peaks ascribed to the TiO<sub>2</sub> film and the Pt layer are, as expected, increased and decreased, respectively, with increasing the thickness of TiO<sub>2</sub> film. More importantly, the results indicate that the crystal structure of TiO<sub>2</sub> does not change with the TiO<sub>2</sub> film thickness. Therefore, the TiO<sub>2</sub> film thickness dependence of the EOP efficiency (Fig. 3) was found not to be due to the change in the crystal structure of TiO<sub>2</sub>.

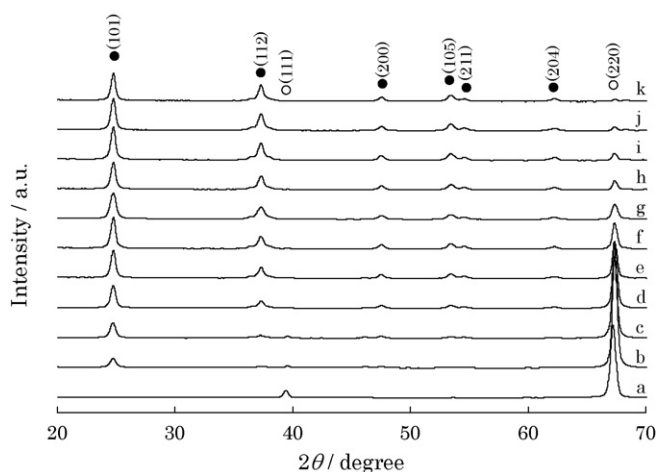


**Fig. 6.** XRD patterns of Si/TiO<sub>x</sub>/Pt/TiO<sub>2</sub> electrodes with different thicknesses of TiO<sub>2</sub> films ((a) 0 nm, (b) 45 nm, (c) 91 nm, (d) 179 nm, (e) 254 nm, (f) 354 nm, (g) 447 nm, (h) 516 nm, (i) 604 nm, (j) 714 nm and (k) 734 nm). Symbols (●) and (○) represent the anatase TiO<sub>2</sub> and Pt peaks, respectively.

Fig. 7 shows the AFM image of a 1  $\mu\text{m} \times 1 \mu\text{m}$  surface (bird's-eye view) of an electrode with a single layer of TiO<sub>2</sub> (the film thickness: ca. 45 nm). It shows the flat nanosheet and the average surface roughness was measured as approximately 1 nm. In addition, using conducting AFM (data not shown), we found that the dark (lower) parts of the image represent the TiO<sub>2</sub>, and therefore, the exposure of the Pt substrate was not observed.

In Fig. 8 are shown the typical TEM images of the cross-sections of the surface TiO<sub>2</sub> films that were fabricated by repeating spin-coating (a) 1, and (b and c) 10 times. Fig. 8(a) demonstrates a typical image of the film structure. Electron diffraction analysis indicates that the particles of the film (approximately 10–20 nm diameters) are crystallized Ti oxides, being in good agreement with the diameters (ca. 20 nm) estimated using Scherrer's equation based on the XRD data. The white parts were also found to be amorphous, and they are ascribed to the epoxy resin used to prepare the samples for the TEM observation. Thus, in fact, the white parts correspond to

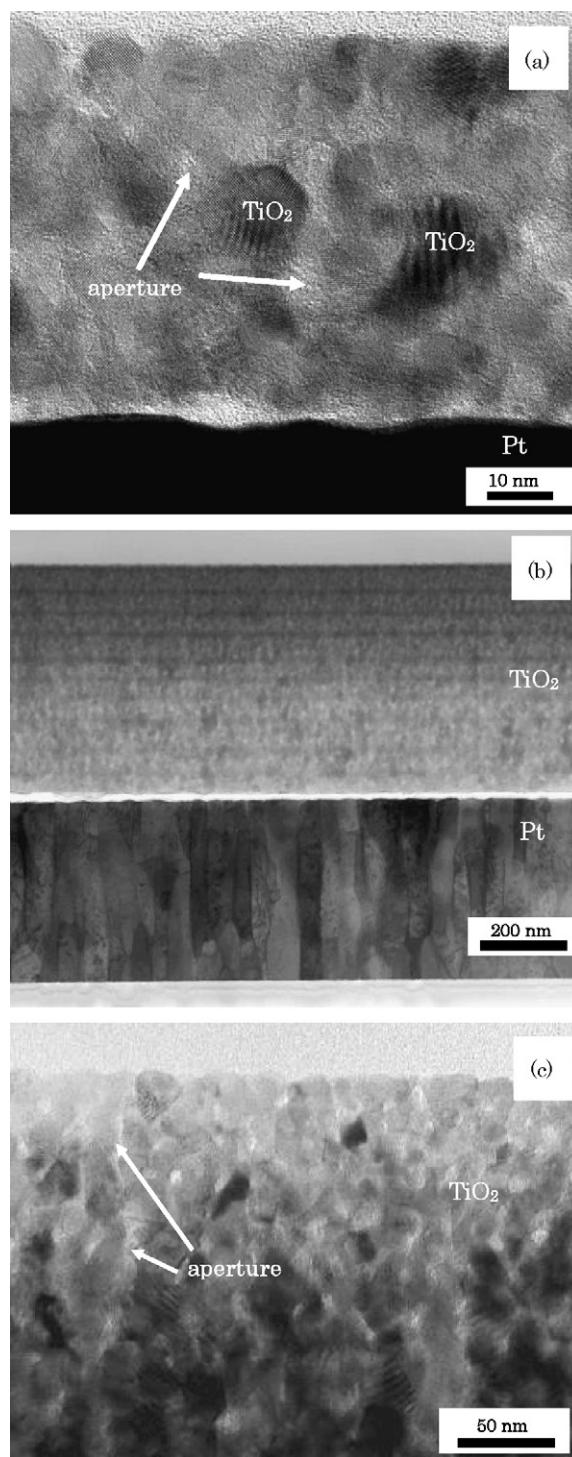


**Fig. 8.** TEM images of the cross-sections of TiO<sub>2</sub> films. Spin-coating: (a) 1 and (b and c) 10 times.

the apertures of the TiO<sub>2</sub> films. The apertures of several nanometers in width shown in Fig. 8(a) appear to form paths from the surface of the TiO<sub>2</sub> film to the Pt substrate. Consequently, the electrolyte solution may penetrate to the Pt substrate through these paths, and the Pt is likely the active site in the electrochemical reaction. This is in agreement with the CV results (Fig. 5). In Fig. 8(b), the structure of the TiO<sub>2</sub> multilayers prepared by repeating spin-coating 10 times is shown. The TiO<sub>2</sub> multilayers were clearly observed to be uniformly fabricated. The belt-shaped white part between the undermost TiO<sub>2</sub> layer and the Pt substrate corresponds to the

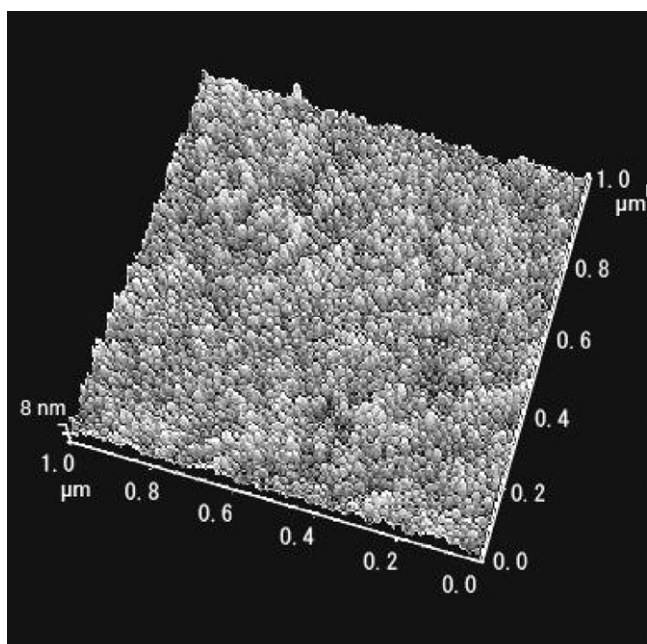


**Fig. 7.** AFM image of a TiO<sub>2</sub> film. Spin-coating: one time.

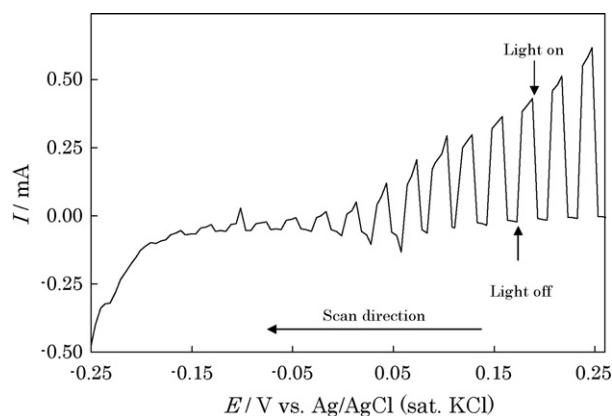


**Fig. 9.** Current–potential curve of a Si/TiO<sub>x</sub>/Pt/TiO<sub>2</sub> electrode (TiO<sub>2</sub> film thickness: 53 nm) under intermittent UV irradiation in 0.1 M HClO<sub>4</sub> at 24 °C. Scan rate: 5 mV s<sup>-1</sup>

exfoliation caused during the preparation of the sample for TEM observation. Fig. 8(c) shows the structure similar to image (a) with the TiO<sub>2</sub> particles of 10–20 nm and apertures of several nanometers. The paths are also shown, but some of them seem to end on the TiO<sub>2</sub> in the depth direction. In the case of Fig. 8(b and c) in which the TiO<sub>2</sub> film was prepared by the 10 times spin-coating and the EOP was observed, the paths seem not to reach the Pt substrate through the thick TiO<sub>2</sub> film from the surface and thus the electrolyte solution does not reach the Pt surface in the electrolysis. Also, the similar multilayered structure was observed for the electrode prepared by repeating spin-coating 18 times (data not shown). Therefore, when the EOP is realized, it is likely that the TiO<sub>2</sub> is the active site for the electrochemical reaction. These TEM observations confirm the electrochemical measurements (Fig. 5).

#### 3.4. Photoelectrochemical measurements

The anatase TiO<sub>2</sub> polycrystalline film is a semiconductor with a band gap ( $E_{bg}$ ) of 3.3 eV [23] and thus the absorption edge corresponding to electron excitation from the valence band is calculated as the wavelength ( $\lambda$ )  $\leq 1240/E_{bg}$  [24], i.e.,  $\sim 376$  nm. Fig. 9 shows the typical photocurrent–potential curve for the TiO<sub>2</sub> spin-coated electrode (thickness: 53 nm) in 0.1 M HClO<sub>4</sub> solution under a chopped UV–vis light irradiation from a Xe lamp ( $180 \text{ nm} \leq \lambda \leq 2000 \text{ nm}$ ). The anodic photocurrent for the OER was observed when the light was illuminated during the anodic polarization and in the dark the current was very small, thus indicating that the TiO<sub>2</sub> film acts as n-type semiconductor electrode. The potential sweep was performed

from anodic to cathodic direction because the peeling of the TiO<sub>2</sub> film from the Pt substrate was observed when the electrode was polarized at more negative potential than approximately  $-0.2 \text{ V}$  vs. Ag/AgCl (sat. KCl). Thus, the onset potential of the photocurrent, i.e., the flat band potential ( $E_{FB}$ ) of this TiO<sub>2</sub> film could not be determined in this measurement.

#### 3.5. Electron transfer scheme for EOP

The electrolysis using TiO<sub>2</sub>-covered electrodes seems to be possible; electrons are transferred via an electron tunneling through the depletion layer of the n-type TiO<sub>2</sub> semiconductor. Because of the aperture structure, the electrolyte solution could penetrate into the inside of the TiO<sub>2</sub> film. Therefore, the actual thickness from the Pt layer to the TiO<sub>2</sub> surface, i.e., the distance from the Pt layer to the site, into which the electrolyte solution could penetrate, in the inside of the TiO<sub>2</sub> film is thinner than the thickness from the Pt layer to the TiO<sub>2</sub> film measured by XRF (Fig. 2). Thus the tunneling current could flow through the thin film at the high bias potentials [25]. The present result that the current efficiency of EOP on the semiconductor (or insulator) corresponding to tunneling current is much higher than that on the Pt substrate itself is in good agreement with our previous work [19].

Fig. 10 shows a schematic illustration of the band structure of the TiO<sub>2</sub>/HClO<sub>4</sub> solution interface of the Si/TiO<sub>x</sub>/Pt/TiO<sub>2</sub> electrode in which the Pt substrate is completely covered with TiO<sub>2</sub>. Fig. 10(a) shows the flat band state of TiO<sub>2</sub> in 0.01 M HClO<sub>4</sub> (pH 2.0) at 298 K. It has been reported that the values of the bottom of the conduction band ( $E_C$ ) and the top of the valence band ( $E_V$ ) for anatase TiO<sub>2</sub> polycrystalline thin film are 4.1 and 7.4 eV vs. vacuum [23], respectively. The relationship between the absolute electron potential of an electrode ( $E_{abs}$ ) and the standard electrode potential (SHE,  $E^\circ$ ) is given by  $E_{abs} = E^\circ + 4.44$ , and the electrode potential changes with solution pH at the rate of  $-0.059 \text{ V/pH}$ . In addition, the potential of Ag/AgCl (sat. KCl) is taken as 0.199 V vs. SHE. Therefore, the values of  $E_C$  and  $E_V$  of TiO<sub>2</sub> in 0.01 M HClO<sub>4</sub> (pH 2.0) are calculated to be  $-0.66$  and  $2.64 \text{ V}$  vs. Ag/AgCl (sat. KCl), respectively.

In the case of a small anodic bias from the flat band state (Fig. 10(b)), the oxidation of water cannot occur because the anodic bias is not enough to oxidize water to produce O<sub>2</sub> and/or O<sub>3</sub>. When a large anodic bias at which ozone production is observed, e.g., 1.98 V vs. Ag/AgCl (sat. KCl) (Fig. 3(c and d)), is applied, the bottom of  $E_C$  of TiO<sub>2</sub> is higher than the oxidation–reduction potential ( $E^\circ$ ) of ozone and it seems that a deep depletion layer is formed on the surface of TiO<sub>2</sub> [25–27]. Therefore, similarly to the case [19] of the EOP using Si/TiO<sub>x</sub>/Pt/TaO<sub>x</sub> electrode, it is considered that in the dark, (i)

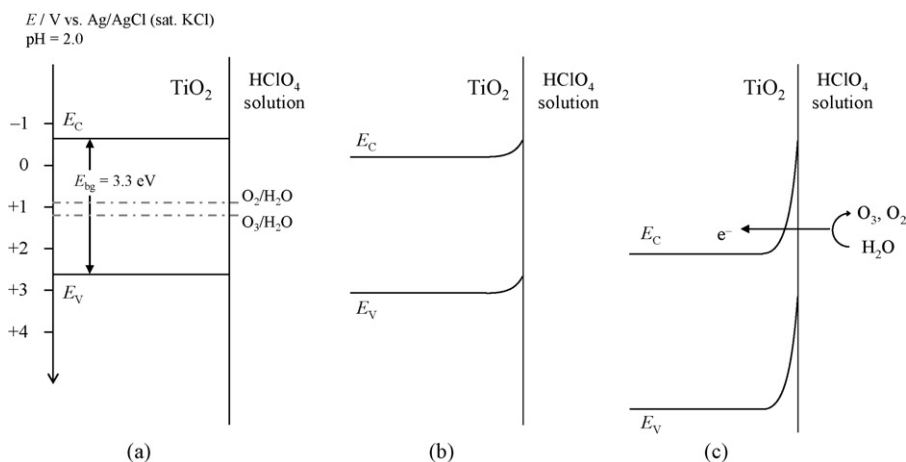


**Fig. 10.** Band models in the TiO<sub>2</sub>/HClO<sub>4</sub> interface in 0.01 M HClO<sub>4</sub> at 298 K under (a) flat band state, (b) anodic bias and (c) external anodic bias.

electrons tunnel through the depletion layer and/or (ii) electrons hop along the interfacial levels in the depletion layer. In both cases, the electron transfer occurs at a more positive potential than the oxidation–reduction potentials of oxygen and ozone. As a result, the OER and/or EOP can take place. From the results shown in Fig. 3 and the above-mentioned tunnel oxidation of water, it should be noted that the Si/TiO<sub>x</sub>/Pt/TiO<sub>2</sub> electrode fabricated in this study is efficient for the EOP probably because of its higher oxygen overpotential, compared with that of the Pt electrode. The high oxygen overpotential is considered to originate from the TiO<sub>2</sub> band structure in which electronic transfer is possible at a high energy level through a deep depletion layer of the TiO<sub>2</sub> surface.

#### 4. Conclusions

EOP could be observed using the Si/TiO<sub>x</sub>/Pt/TiO<sub>2</sub> electrodes covered with spin-coated TiO<sub>2</sub> films of more than 440 nm in 0.01 M HClO<sub>4</sub> at 15 °C and the current efficiency of ca. 7% was achieved at a current density of 26.7 mA cm<sup>-2</sup>. According to the electrochemical measurements and EOP experiments, the electrodes in which the exposure of the Pt substrate was not observed could generate ozone. The TiO<sub>2</sub> films were found to be of anatase and have the structures with TiO<sub>2</sub> particles and apertures. The photoelectrochemical measurements revealed that the TiO<sub>2</sub> films were of n-type semiconductors. The band structure of the TiO<sub>2</sub>/HClO<sub>4</sub> interface accounts for electron transfer at a high bias potential, which is profitable for EOP through the depletion layer of the n-type semiconductor TiO<sub>2</sub>, as tunneling current.

#### Acknowledgement

The authors would like to thank Drs. Tsutomu Minegishi, Jun Kubota and Kazunari Domen at the University of Tokyo for their skillful assistance with the photoelectrochemical measurements.

#### References

- [1] L.M. Da Silva, L.A. De Faria, J.F.C. Boodts, *Pure Appl. Chem.* 73 (2001) 1871.
- [2] L.M. Da Silva, M.H.P. Santana, J.F.C. Boodts, *Quim. Nova* 26 (2003) 880.
- [3] P.C. Foller, C.W. Tobias, *J. Electrochem. Soc.* 129 (1982) 506.
- [4] S. Trasatti, *Int. J. Hydrogen Energy* 20 (1995) 835.
- [5] R. Amadelli, A. De Battisti, D.V. Girenko, S.V. Kovalyov, A.B. Velichenko, *Electrochim. Acta* 46 (2000) 341.
- [6] R. Amadelli, A. Maldotti, A. Molinari, F.I. Danilov, A.B. Velichenko, *J. Electroanal. Chem.* 534 (2002) 1.
- [7] L.M. Da Silva, L.A. De Faria, J.F.C. Boodts, *Electrochim. Acta* 48 (2003) 699.
- [8] E.R. Kötz, S. Stucki, *J. Electroanal. Chem.* 228 (1987) 407.
- [9] D.V. Franco, L.M. Da Silva, W.F. Jardim, J.F.C. Boodts, *J. Braz. Chem. Soc.* 17 (2006) 746.
- [10] D.M. Shub, M.F. Reznik, *Elektrokhimiya* 21 (1985) 855.
- [11] M.H. Miles, E.A. Klaus, B.P. Gunn, J.R. Locker, W.E. Serafin, *Electrochim. Acta* 23 (1978) 521.
- [12] K. Arihara, C. Terashima, A. Fujishima, *J. Electrochem. Soc.* 154 (2007) E71.
- [13] M.H.P. Santana, L.A. De Faria, J.F.C. Boodts, *Electrochim. Acta* 49 (2004) 1925.
- [14] L.M. Da Silva, D.V. Franco, L.A. De Faria, J.F.C. Boodts, *Electrochim. Acta* 49 (2004) 3977.
- [15] K. Kaneda, M. Ikematsu, Y. Koizumi, H. Minooshima, T. Rakuma, D. Takaoka, M. Yasuda, *Electrochem. Solid State Lett.* 8 (2005) J13.
- [16] M.I. Awad, S. Sata, K. Kaneda, M. Ikematsu, T. Okajima, T. Ohsaka, *Electrochem. Commun.* 8 (2006) 1263.
- [17] K. Kaneda, M. Ikematsu, M. Iseki, D. Takaoka, T. Higuchi, T. Hattori, T. Tsukamoto, M. Yasuda, *Jpn. J. Appl. Phys. Part 1: Regul. Pap. Brief Commun. Rev. Pap.* 45 (2006) 5154.
- [18] K. Kaneda, M. Ikematsu, M. Iseki, D. Takaoka, T. Higuchi, T. Hattori, T. Tsukamoto, M. Yasuda, *Chem. Lett.* 34 (2005) 1320.
- [19] K. Kaneda, M. Ikematsu, K. Kitsuka, M. Iseki, H. Matsuura, T. Higuchi, T. Hattori, T. Tsukamoto, M. Yasuda, *Jpn. J. Appl. Phys. Part 1: Regul. Pap. Brief Commun. Rev. Pap.* 45 (2006) 6417.
- [20] A.M. Mohammad, K. Kitsuka, K. Kaneda, M.I. Awad, A.M. Abdullah, M. Ikematsu, T. Ohsaka, *Chem. Lett.* 36 (2007) 1046.
- [21] J. Newman, *J. Electrochem. Soc.* 117 (1970) 507.
- [22] A.M. Schmidt, D.S. Azambuja, E.M.A. Martini, *Corros. Sci.* 48 (2006) 2901.
- [23] G.M. Liu, W. Jaegermann, J.J. He, V. Sundstrom, L.C. Sun, *J. Phys. Chem. B* 106 (2002) 5814.
- [24] R. Kun, M. Szekeres, I. Dekany, *Appl. Catal. B: Environ.* 68 (2006) 49.
- [25] S. Ohkubo, Y. Ashida, I. Utsumi, K. Hongo, G. Nogami, *J. Electrochem. Soc.* 143 (1996) 3273.
- [26] D. Vanmaekelbergh, *Electrochim. Acta* 42 (1997) 1121.
- [27] G. Nogami, H. Sei, A. Aoki, S. Ohkubo, Y. Hamasaki, *J. Electrochem. Soc.* 141 (1994) 3410.